Apparent conflicting Roadian–Wordian (middle Permian) CA-IDTIMS and palynology ages from the Canning Basin, Western Australia

A. J. Mory[a,b], J. L. Crowley[c], J. Backhouse[b], R. S. Nicoll[d,e], S. E. Bryan[f], M. López Martínez[g] and D. J. Mantle[h]

[a] Geological Survey of Western Australia, 100 Plain St, East Perth, WA 6004, Australia

[b] UWA Centre for Energy Geoscience, School of Earth and Environment (M004), The University of Western Australia, 35 Stirling Highway, Crawley, WA 6009, Australia

[c] Department of Geosciences, 1910 University Drive, Boise State University, Boise, ID 83725-1535, USA

[d] Geoscience Australia, GPO Box 378, Canberra, ACT 2601, Australia

[e] Research School of Earth Sciences, Australian National University, Building 142, Mills Road, Acton, ACT 2601, Australia

[f] Queensland University of Technology, School of Earth, Environmental and Biological Sciences, GPO Box 2434 Brisbane, Queensland 4001, Australia

[g] Departamento de Geología, Centro de Investigación Científica y de Educación Superior de Ensenada, Carretera Ensenada-Tijuana No 3918, 22860, Ensenada, Baja California, México

[h] MGPalaeo, Unit 1, 5 Arvida St, Malaga WA 6090, Australia

Australian Journal of Earth Sciences (2017) *64 (7),*
http://dx.doi.org/10.1080/08120099. 2017.1365586

Supplementary papers

Appendix 1 Palynology summary.

Table A1.1 Summary range chart and palynozonation for Pittston SD-1

Table A1.2 Summary range chart and palynozonation for Rey Resources drill holes

Appendix 2 Core tray images of 619.5–654.5 m, Pittston SD-1

Figure A2 Core tray images for 619.5–645.5 m showing main interval of interest and positions of tuffaceous beds that yielded zircon ages

Appendix 3 Zircon geochronology methods.

Table A3.1. LA-ICPMS zircon isotopic U–Pb and trace element concentration data for Pittston SD-1

Table A3.2. CA-IDTIMS U–Pb zircon isotopic data for Pittston SD-1

Appendix 4 Ar–Ar dating method.

Table A4 Ar–Ar data for sample 711.85–711.95 m from Pittston SD-1.

Appendix 1

Palynology summary

A summary of the palynology methods followed for this paper is given in the supplementary papers to Laurie et al. (2016) with the only difference being that the SD-1 samples were processed at The University of Western Australia (Crawley, Western Australia) palynology laboratory in the School of Earth and Environment. Palynostratigraphic results and zonal determinations for samples from Pittston SD-1 and Rey Resources core are presented in Tables A1.1 and A1.2, respectively. The palynological zonal scheme adopted follows Backhouse (1991, 1993) for Permian biostratigraphic studies in the onshore Western Australian basins. Equivalent eastern Australian zones follow the alphanumeric hierarchical scheme of Price et al. (1985) and Price (1997).

Table A1.1. Summary range chart and palynozonation for Pittston SD-1. (Excel spreadsheet)
Table A1.2. Summary range chart and palynozonation for Rey Resources drill holes. (Excel spreadsheet)

Appendix 2

Core tray images of 619.5–654.5 m, Pittston SD-1

The images are from the HyLogger database at the Geological Survey of Western Australia and cover the main interval containing tuffaceous beds (621–643.5 m) that have been dated for this paper. The three beds that yielded datable zircons (Appendix 3) are marked on the image as is the disconformity at 621 m (A) between heterolithic facies within the *D. parvithola* Zone (above) and the coaly siltstone with thin tuffaceous beds within the *M. villosa* Zone (below, see Appendix 1). The base of the interval is placed at 643.5 m (B) just below a basalt fragment in the basal tuff. Note that it is unclear if the depth blocks in the core tray were placed by the drillers or were moved to account for discrepancies between the interval drilled and the core recovered for each core run. Consequently, the depths assigned when the core was scanned by the HyLogger are not necessarily accurate.

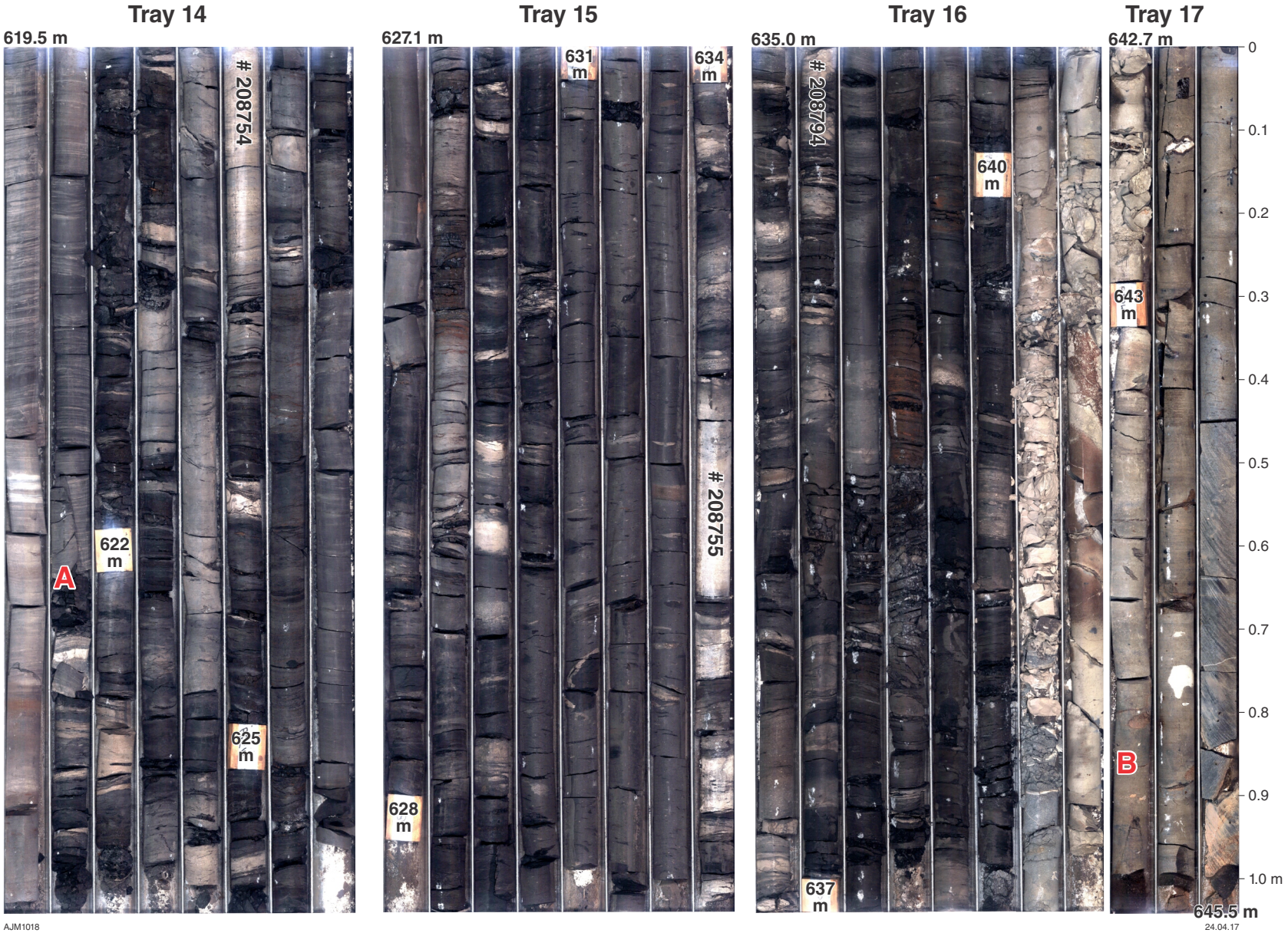

Figure A2. Core tray images for 619.5–645.5 m showing main interval of interest (A–B) and tuffaceous beds that yielded zircon ages.

Appendix 3

Zircon geochronology methods

The U–Pb zircon geochronology methods followed for this paper are similar to those followed by Laurie et al. (2016). The SD-1 samples were also prepared and analysed at Boise State University (Boise, Idaho, USA). The position of the three productive tuffaceous samples is shown in Appendix 2.

LA-ICPMS

Zircon grains were separated from rocks using standard techniques, annealed at 900ºC for 60 hours in a muffle furnace, and mounted in epoxy and polished until their centres were exposed. Cathodoluminescence (CL) images were obtained with a JEOL JSM-1300 scanning electron microscope and Gatan MiniCL. Zircon was analysed by laser ablation inductively coupled plasma mass spectrometry (LA-ICPMS) using a ThermoElectron X-Series II quadrupole ICPMS and New Wave Research UP-213 Nd:YAG UV (213 nm) laser ablation system. In-house analytical protocols, standard materials, and data reduction software were used for acquisition and calibration of U–Pb dates and a suite of high field strength elements (HFSE) and rare earth elements (REE). Zircon was ablated with a laser spot of 25 μm width using fluence and pulse rates of 5 J/cm^2 and 10 Hz, respectively, during a 45 second analysis (15 sec gas blank, 30 sec ablation) that excavated a pit ~25 μm deep. Ablated material was carried by a 1.2 L/min He gas stream to the nebulizer flow of the plasma. Dwell times were 5 ms for Si and Zr, 200 ms for ^{49}Ti and ^{207}Pb, 80 ms for ^{206}Pb, 40 ms for ^{202}Hg, ^{204}Pb, ^{208}Pb, ^{232}Th and ^{238}U and 10 ms for all other HFSE and REE. Background count rates for each analyte were obtained prior to each spot analysis and subtracted from the raw count rate for each analyte. Ablations pits that intersect glass or mineral inclusions (identified based on Ti and P. U–Pb dates) are considered valid if the U–Pb ratios appear to be unaffected by the inclusions. Analyses were rejected where ^{204}Pb was elevated above the baseline suggesting contamination by common Pb. For concentration calculations, background-subtracted count rates for each analyte were internally normalized to ^{29}Si and calibrated with respect to NIST SRM-610 and -612 glasses as the primary standards. Temperature was calculated from the Ti-in-zircon thermometer (Watson et al., 2006). Because there are no constraints on the activity of TiO_2, an average value in crustal rocks of 0.8 was used.

Data were collected in one experiment in October 2014. For U–Pb and ^{207}Pb/^{206}Pb dates, instrumental fractionation of the background-subtracted ratios was corrected and dates were calibrated with respect to interspersed measurements of zircon standards and reference materials. The primary standard Plešovice zircon (Sláma et al., 2008) was used to monitor time-dependent instrumental fractionation based on two analyses for every 10 analyses of unknown zircon. A secondary correction to the ^{206}Pb/^{238}U dates was made based on results from the zircon standard Seiland (530 Ma, unpublished data, Boise State University), which was treated as an unknown and measured once for every 10 analyses of unknown zircon. These results showed a linear age bias of up to 2% that is related to the ^{206}Pb count rate. The secondary correction is thought to mitigate matrix-dependent variations due to contrasting compositions and ablation characteristics between the Plešovice zircon and other standards (and unknowns).

Radiogenic isotope ratio and age error propagation for all analyses includes uncertainty contributions from counting statistics and background subtraction. For groups of analyses that are collectively interpreted from a weighted mean date (i.e., igneous zircon analyses), a weighted mean date was first calculated using Isoplot 3.0 (Ludwig, 2003) using errors on individual dates, which do not include a standard calibration uncertainty, and then a standard calibration uncertainty was propagated into the error on the weighted mean date. This uncertainty is the local standard deviation of the polynomial fit to the interspersed primary standard measurements versus time for the time-dependent, relatively larger U/Pb fractionation factor, and the standard error of the mean of the consistently time-invariant and smaller $^{207}Pb/^{206}Pb$ fractionation factor. These uncertainties are 2.3% (2σ) for $^{206}Pb/^{238}U$ and 0.7% (2σ) for $^{207}Pb/^{206}Pb$. Age interpretations are based on $^{207}Pb/^{206}Pb$ dates. Errors on the $^{207}Pb/^{206}Pb$ and $^{206}Pb/^{238}U$ dates from individual analyses are given at 2σ, as are the errors on the weighted mean dates.

CA-IDTIMS U–Pb geochronology

U–Pb dates were obtained by the chemical abrasion isotope dilution thermal ionization mass spectrometry (CA-IDTIMS) method from analyses composed of single zircon grains (Table A.3), modified after Mattinson (2005). Zircon was separated from rocks using standard techniques, placed in a muffle furnace at 900°C for 60 hours in quartz beakers, mounted in epoxy, and polished until the centres of the grains were exposed. Cathodoluminescence (CL) images were obtained with a JEOL JSM-1300 scanning electron microscope and Gatan MiniCL. LA-ICPMS was performed on sample 208754. Zircon was removed from the epoxy mounts for dating based on CL images and LA-ICPMS data.

Single grains were put into 3 ml Teflon PFA beakers and loaded into 300 μl Teflon PFA microcapsules. Fifteen microcapsules were placed in a large-capacity Parr vessel and the grains partially dissolved in 120 μl of 29 M HF for 12 hours at 180°C. The contents of the microcapsules were returned to 3 ml Teflon PFA beakers, HF removed, and the residual grains immersed in 3.5 M HNO_3, ultrasonically cleaned for an hour, and fluxed on a hotplate at 80°C for an hour. The HNO_3 was removed and grains were rinsed twice in ultrapure H_2O before being reloaded into the 300 μl Teflon PFA microcapsules (rinsed and fluxed in 6 M HCl during sonication and washing of the grains) and spiked with the EARTHTIME mixed $^{233}U–^{235}U–^{205}Pb$ tracer solution. Zircon was dissolved in Parr vessels in 120 μl of 29 M HF with a trace of 3.5 M HNO_3 at 220°C for 48 hours, dried to fluorides, and re-dissolved in 6 M HCl at 180°C overnight. U and Pb were separated from the zircon matrix using an HCl-based anion-exchange chromatographic procedure (Krogh, 1973), eluted together and dried with 2 μl of 0.05 N H_3PO_4.

Pb and U were loaded on a single outgassed Re filament in 5 μl of a silica-gel/phosphoric acid mixture (Gerstenberger & Haase, 1997), and U and Pb isotopic measurements made on a GV Isoprobe-T multicollector thermal ionization mass spectrometer equipped with an ion-counting Daly detector. Pb isotopes were measured by peak-jumping all isotopes on the Daly detector for 160 cycles, and corrected for 0.16 ± 0.03%/a.m.u. (1 sigma error) mass fractionation. Transitory isobaric interferences due to high-molecular weight organics, particularly on ^{204}Pb and ^{207}Pb, disappeared within

approximately 30 cycles, while ionization efficiency averaged 10^4 cps/pg of each Pb isotope. Linearity (to ≥1.4 x 10^6 cps) and the associated dead-time correction of the Daly detector were monitored by repeated analyses of NBS982, and have been constant since installation. Uranium was analysed as UO_2+ ions in static Faraday mode on 10^{12} ohm resistors for 300 cycles, and corrected for isobaric interference of $^{233}U^{18}O^{16}O$ on $^{235}U^{16}O^{16}O$ with an $^{18}O/^{16}O$ of 0.00206. Ionization efficiency averaged 20 mV/ng of each U isotope. U mass fractionation was corrected using the known $^{233}U/^{235}U$ ratio of the EARTHTIME tracer solution.

U–Pb dates and uncertainties were calculated using the algorithms of Schmitz & Schoene (2007), EARTHTIME ET535 tracer solution (Condon et al., 2015) with calibration of $^{235}U/^{205}Pb$ = 100.233, $^{233}U/^{235}U$ = 0.99506, and $^{205}Pb/^{204}Pb$ = 11268, and U decay constants recommended by Jaffey et al. (1971). $^{206}Pb/^{238}U$ ratios and dates were corrected for initial ^{230}Th disequilibrium using a $Th/U_{[magma]}$ = 3.0 ± 0.3 (1σ) using the algorithms of Crowley et al. (2007), resulting in an increase in the $^{206}Pb/^{238}U$ dates of ca 0.09 Ma. All common Pb in analyses was attributed to laboratory blank and subtracted based on the measured laboratory Pb isotopic composition and associated uncertainty. U blanks are estimated at 0.020 ± 0.010 pg (1σ).

Weighted mean $^{206}Pb/^{238}U$ dates were calculated from equivalent dates using Isoplot 3.0 (Ludwig, 2003). Errors on the weighted mean dates are given as ± x / y / z, where x is the internal error based on analytical uncertainties only, including counting statistics, subtraction of tracer solution, and blank and initial common Pb subtraction, y includes the tracer calibration uncertainty propagated in quadrature, and z includes the ^{238}U decay constant uncertainty propagated in quadrature. Internal errors should be considered when comparing our dates with $^{206}Pb/^{238}U$ dates from other laboratories that used the same EARTHTIME tracer solution or a tracer solution cross-calibrated using EARTHTIME gravimetric standards. Errors including the uncertainty in the tracer calibration should be considered when comparing our dates with those derived from other geochronological methods using the U–Pb decay scheme (e.g., laser ablation ICPMS). Errors including uncertainties in the tracer calibration and ^{238}U decay constant (Jaffey et al., 1971) should be considered when comparing our dates with those derived from other decay schemes (e.g., $^{40}Ar/^{39}Ar$, $^{187}Re–^{187}Os$). Errors for weighted mean dates and dates from individual grains are given at 2σ.

Table A3.1. LA-ICPMS zircon isotopic U–Pb and trace element concentration data for Pittston SD-1. (Excel spreadsheet)

Table A3.2. CA-IDTIMS U–Pb zircon isotopic data for Pittston SD-1. (Excel spreadsheet)

Appendix 4

Ar–Ar dating methodology

The methodology commenced with step-heating experiments on a Coherent Innova 300 Ar-ion laser beam followed by the determination of argon isotopes with a VG5400 mass spectrometer. The samples received 120 MW at position 8C of McMaster University nuclear reactor at Hamilton, Ontario, Canada. The irradiation monitor used was sanidine FCT 2 (28.201 ± 0.046 Ma; Kuiper et al., 2008). The samples and irradiation monitor were covered with a Cd liner to block thermal neutrons.

Each argon isotopic experiment is preceded by a blank to measure the Ar background of the system. All argon isotopes are determined for the blank and the sample. The laser power is incremented sequentially to release the argon during the step heating experiments. The laser power used for each step is given in the first column of the table, followed by the size of the ^{39}Ar signal in microvolts and as percentage. The $^{40}Ar^*/^{39}Ar_K$ value given is corrected for: blank; nuclear interference reactions due to Ca, K and Cl; mass discrimination of the mass spectrometer; and radioactive decay of ^{37}Ar and ^{39}Ar. For the ages given in the table and the age spectrum presented in the figure it is assumed that $(^{40}Ar/^{36}Ar)_i = 295.5$.

The decay constants and isotopic compositions recommended by Steiger & Jäger (1977) were used in all the calculations. For the interference reactions the factors used were: $(^{39}Ar/^{37}Ar)_{Ca} = 6.50 \times 10^{-4}$; $(^{36}Ar/^{37}Ar)_{Ca} = 2.55 \times 10^{-4}$; $(^{40}Ar/^{39}Ar)_K = 0$. Additionally, mass 36 was corrected for Cl interference following the reaction ^{36}Ar (^{35}Cl (n, γ) $^{36}Cl \rightarrow {}^{36}Ar + \beta$ with a ^{36}Cl half-life of 3.1×10^5 a). For each fraction, the percentage of radiogenic ^{40}Ar ($^{40}Ar^*$), the $^{40}Ar/^{36}Ar$ ratio and the $^{37}Ar_{Ca}/^{39}Ar_K$ representative of the Ca/K ratio are given in Table A.4.

The integrated results of each experiment are calculated adding the signal of the argon isotopes of each fraction. The J value is calculated with the weighted mean of several one-step fusion experiments performed on the irradiation monitor closest to the sample. The equations given by York et al. (2004) were used in all the straight-line calculations.

Table A4. Ar–Ar data for sample 711.85–711.95 m from Pittston SD-1 (Excel spreadsheet)

References

Backhouse, J. (1991). Permian palynostratigraphy of the Collie Basin, Western Australia. *Review of Palaeobotany and Palynology, 67*, 237–314. doi:10.1016/0034-6667(91)90046-6

Backhouse, J. (1993). *Palynology and correlation of Permian sediments in the Perth, Collie and Officer Basins, Western Australia.* Perth WA: Geological Survey of Western Australia, Report 34, 111–128. http://dmpbookshop.eruditetechnologies.com.au/product/palynology-and-correlation-of-permian-sediments-in-the-perth-collie-and-officer-basins-western-australia.do

Condon, D. J., Schoene, B., McLean, N. M., Bowring, S. A., & Parrish, R. (2015). Metrology and traceability of U–Pb isotope dilution geochronology (EARTHTIME Tracer Calibration Part I). *Geochimica et Cosmochimica Acta, 164,* 464–480. doi.org/10.1016/j.gca.2015.05.026

Crowley, J. L., Schoene, B., & Bowring, S. A. (2007). U–Pb dating of zircon in the Bishop Tuff at the millennial scale. *Geology, 35*, 1123–1126. doi: 10.1130/G24017A.1

Gerstenberger, H., & Haase, G. (1997). A highly effective emitter substance for mass spectrometric Pb isotope ratio determinations. *Chemical Geology, 136*, 309–312. doi.org/10.1016/S0009-2541(96)00033-2

Jaffey, A. H., Flynn, K. F., Glendenin, L. E., Bentley, W. C., & Essling, A. M. (1971). Precision measurements of half-lives and specific activities of ^{235}U and ^{238}U. *Physical Review C, 4*, 1889–1906. doi:10.1103/PhysRevC.4.1889

Krogh, T. E. (1973). A low-contamination method for hydrothermal decomposition of zircon and extraction of U and Pb for isotopic age determination. *Geochimica et Cosmochimica Acta, 37*, 485–494. doi.org/10.1016/0016-7037(73)90213-5

Kuiper, K. F., Deino, A., Hilgen, F. J., Krijgsman, W., Renne, P. R., & Wijbrans, J. R. (2008). Synchronizing rock clocks of Earth history. *Science 320 (5875)*, 500–504. doi:10.1126/science.1154339

Laurie, J. R., Bodorkos, S., Nicoll, R. S., Crowley, J. L., Mantle, D. J., Mory, A. J., Wood, G. R., Backhouse, J., Holmes, E. K., Smith T. E., & Champion, D. C. (2016). Calibrating the middle and late Permian palynostratigraphy of Australia to the geologic time-scale via U–Pb zircon CA-IDTIMS dating. *Australian Journal of Earth Sciences*, *63 (6)*, 701–730. doi:10.1080/08120099.2016.1233456

Ludwig, K. R. (2003). User's Manual for Isoplot 3.00. Berkeley Geochronology Center, Special Publication No. 4, Berkeley, CA, 70 p.

Mattinson, J. M. (2005). Zircon U–Pb chemical abrasion ("CA-TIMS") method: combined annealing and multi-step partial dissolution analysis for improved precision and accuracy of zircon ages. *Chemical Geology, 220*, 7–66. doi.org/10.1016/j.chemgeo.2005.03.011

Price, P. L. (1997). Permian to Jurassic palynostratigraphic nomenclature of the Bowen and Surat basins. In P. M. Green (Ed.), *The Surat and Bowen Basins, south-east Queensland* (pp. 137–178). Brisbane, Qld: Queensland Minerals and Energy, Review Series, 9.

Price, P. L., Filatoff, J., Williams, A. J., Pickering, S. A., & Wood, G. R. (1985). Late Palaeozoic and Mesozoic palynostratigraphical units. *CSR Oil and Gas Division Report, 274/25* (QDEX Report Number 14012). Retrieved from https://qdexguest.dnrm.qld.gov.au/portal/site/qdex/

Schmitz, M. D., & Schoene, B. (2007). Derivation of isotope ratios, errors and error correlations for U–Pb geochronology using ^{205}Pb–^{235}U–(^{233}U)-spiked isotope dilution thermal ionization mass spectrometric data: *Geochemistry, Geophysics, Geosystems (G3) 8*, Q08006. doi:10.1029/2006GC001492

Sláma, J., Košler, J., Condon, D. J., Crowley, J. L., Gerdes, A., Hanchar, J. M., Horstwood, M. S. A., Morris, G. A., Nasdala, L., Norberg, N., Schaltegger, U., Schoene, B., Tubrett, M. N, & Whitehouse, M. J. (2008). Plešovice zircon — A new natural reference material for U–Pb and Hf isotopic microanalysis. *Chemical Geology, 249,* 1–35. doi.org/10.1016/j.chemgeo.2007.11.005

Steiger, R. H., & Jäger, E. (1977). Subcommission on geochronology: Convention on the use of decay constants in geo- and cosmochronology. *Earth and Planetary Science Letters 36*, 359–362. doi.org/10.1016/0012-821X(77)90060-7

Watson, E. B., Wark, D. A., & Thomas, J. B. (2006). Crystallization thermometers for zircon and rutile. *Contributions to Mineralogy and Petrology, 151,* 413–433. doi:10.1007/s00410-006-0068-5

York, D., Evensen, N. M., López-Martínez, M., & De Basabe, J. D. (2004). Unified equations for the slope, intercept, and standard errors of the best straight line. *American Journal of Physics 72*, 367–375. doi:10.1119/1.1632486